Supplementary Information (SI) for Journal of Materials Chemistry A.

Supporting Information

Two-dimensional self-assembled $TiSe_2$ micro-nanoparticles toward high-performance sodium ions storage

Jiaxin Liu[1], Shenghong Yang[1], Rui Jiang[1], Lu Yu[1], Shilin Zhou[1], Xiaoyan Shi[1], Junling Xu[1], Lianyi Shao[1]*, Zhipeng Sun[1]*, and Lifeng Hang[2]*

[1]School of Materials and Energy, Guangdong University of Technology, Guangzhou 510006, Guangdong, China.

[2]Department of Medical Imaging, Guangdong Second Provincial General Hospital, Guangzhou 518037, Guangdong, China.

E-mail: shaolianyi@gdut.edu.cn, zpsunxj@gdut.edu.cn, hanglf@ustc.edu.cn.

Material Characterizations. X-ray powder diffraction (XRD, Rigaku SmartLab diffractometer with Cu kα radiation, λ=1.5418 Å) was used to detect the phase composition and crystallinity of the samples. X-ray photoelectron spectroscopy (XPS, Thermo Fisher ESCALAB250Xi) was applied to determine the surface element composition and analyze the valence state of the samples. High resolution transmission electron microscopy (HRTEM, Talos F200S) and scanning electron microscopy (SEM, JEOL-6300F) were carried out to characterize the micro-structure and morphology of the samples. Thermogravimetric (TG, 1600HT) analyzer was used to determine the thermal stability of $TiSe_2$. Nitrogen adsorption–desorption isotherms were carried out on a Micromeritics ASAP2460 instrument to identify the specific surface area. Contact angle meter (JY-PHc) was used to determine the degree of infiltration between the electrode and the electrolyte.

Electrochemical measurements. The sample, superconducting carbon black, and sodium carboxymethyl cellulose (CMC-Na) were mixed uniformly in deionized water with the weight ratio of 7:2:1. The electrode slurry was next pasted homogeneously on a copper foil and then dried at 60 °C for 12 h. The dried copper foil was cut into discs with a diameter of 12 mm as the anode electrode. A sodium disc was chosen as the counter electrode, while a 1.0 M solution of sodium hexafluorophosphate ($NaPF_6$) dissolved in diglyme was employed as the electrolyte. The coin cells were assembled using these components in an argon-filled glovebox. The galvanostatic charge-discharge (GCD) test was performed on the NEWARE battery test system within a voltage range of 1–3 V. Cyclic voltammetry (CV) curves and electrochemical impedance spectroscopy (EIS) were both collected on the electrochemical workstation (CHI 660E).

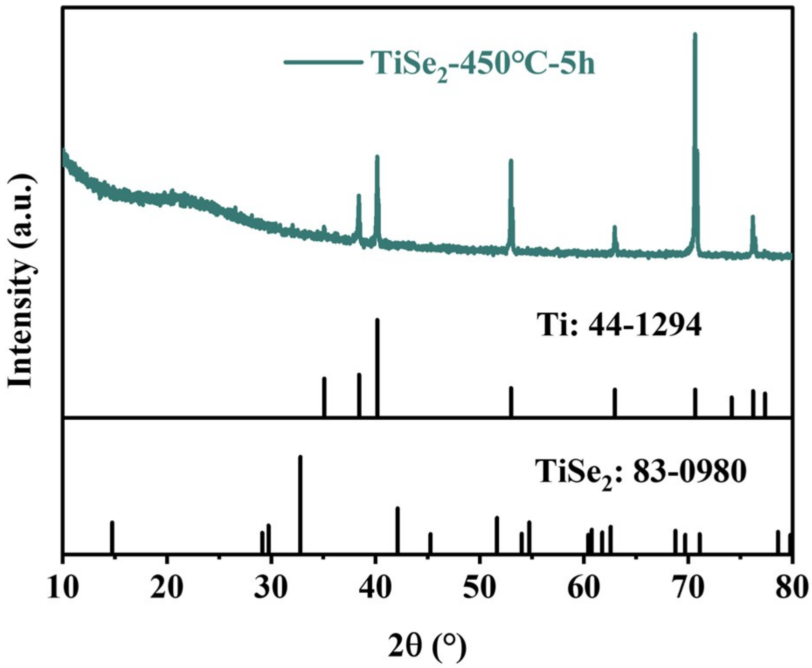

Figure S1. XRD pattern of $TiSe_2$-450°C-5h.

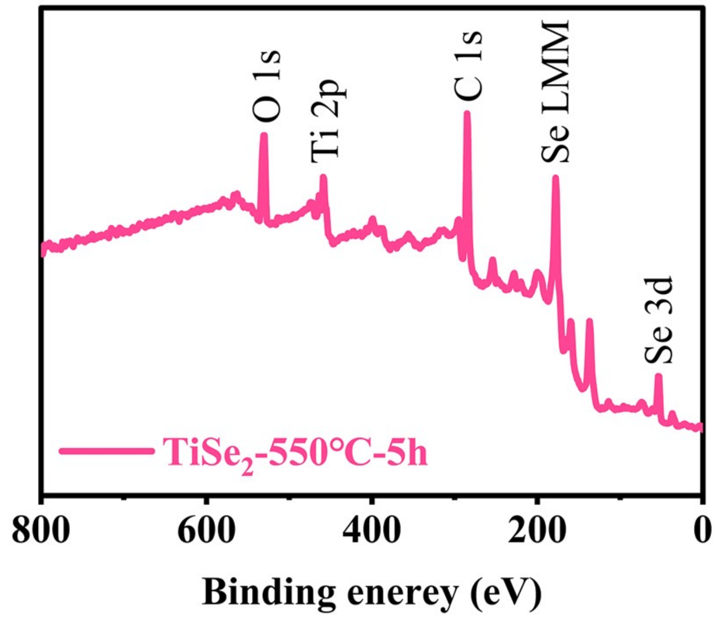

Figure S2. XPS full spectrum of $TiSe_2$-550°C-5h.

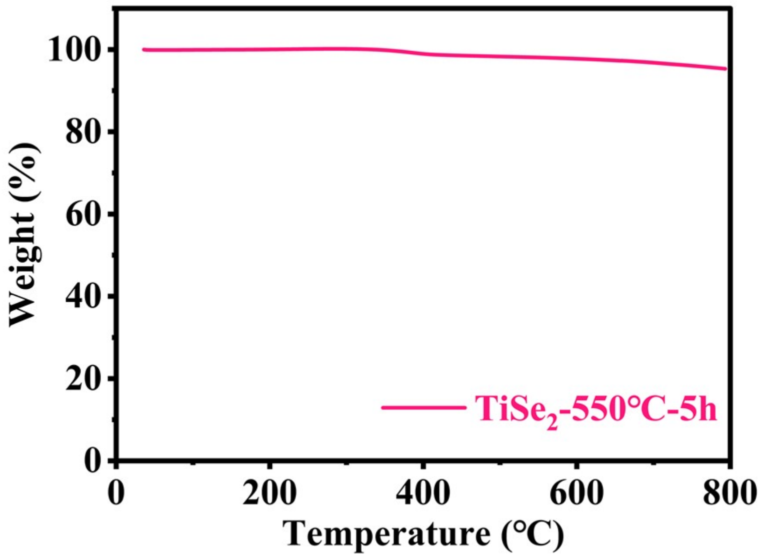

Figure S3. TG curve of $TiSe_2$-550°C-5h.

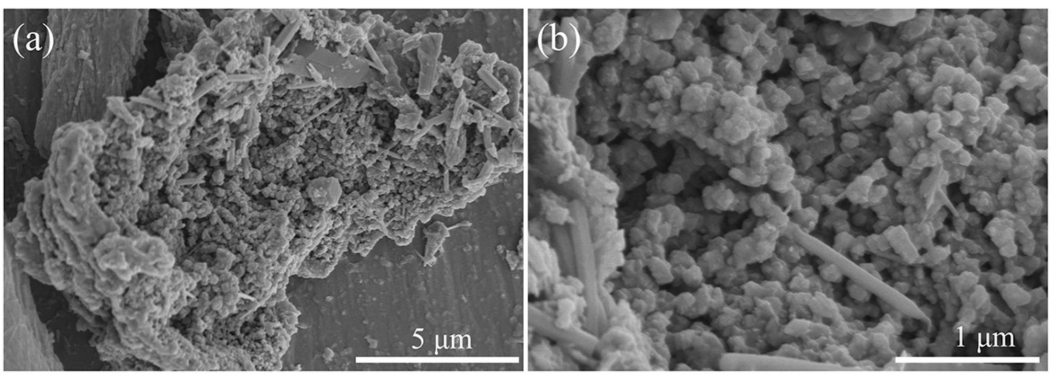

Figure S4. SEM images of $TiSe_2$-450°C-5h.

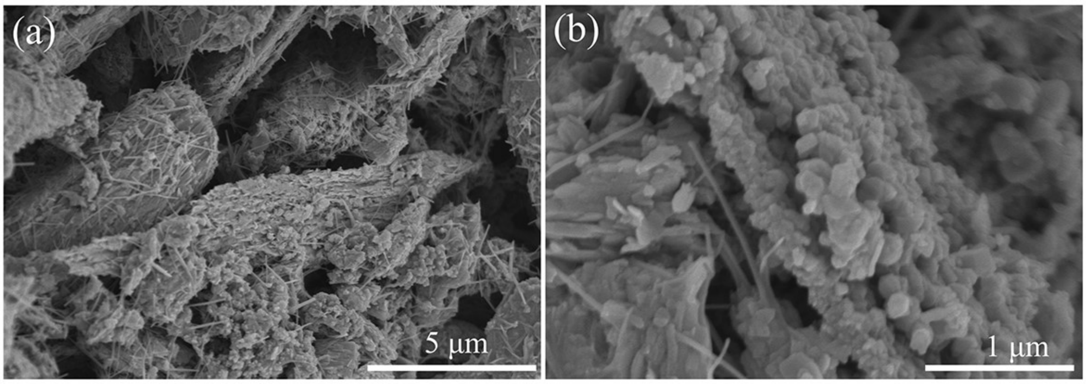

Figure S5. SEM images of $TiSe_2$-550℃-2h.

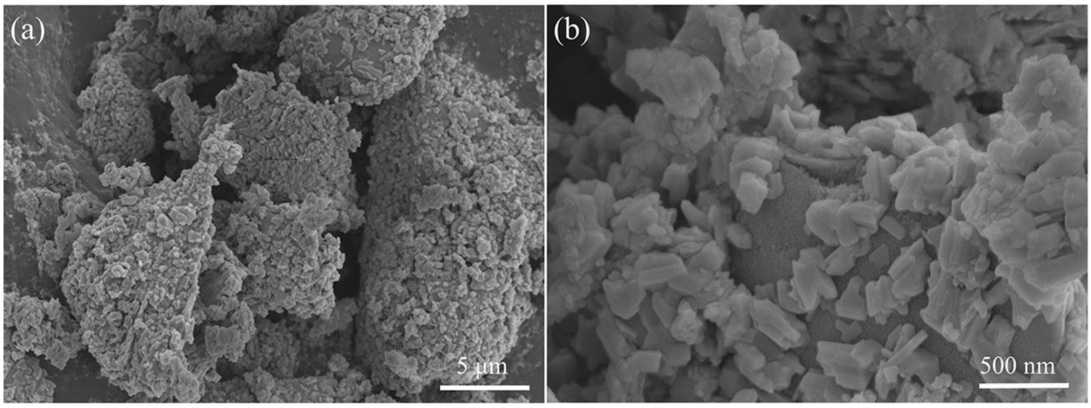

Figure S6. SEM images of $TiSe_2$-650℃-5h.

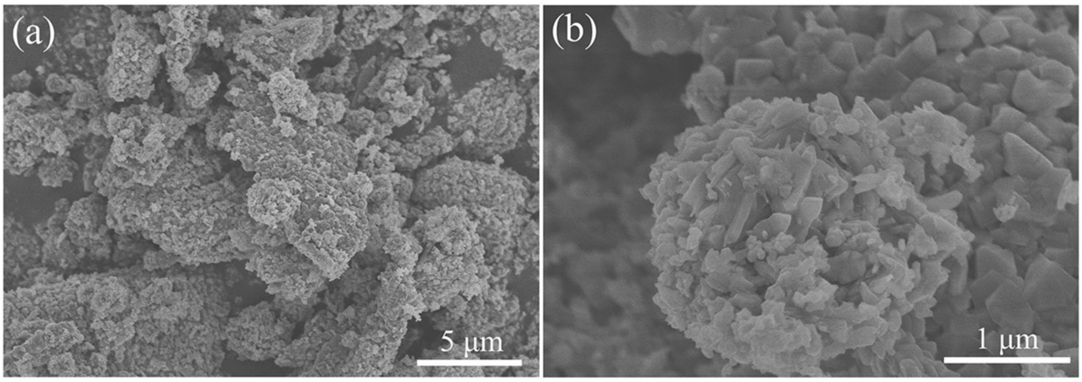

Figure S7. SEM images of $TiSe_2$-550℃-8h.

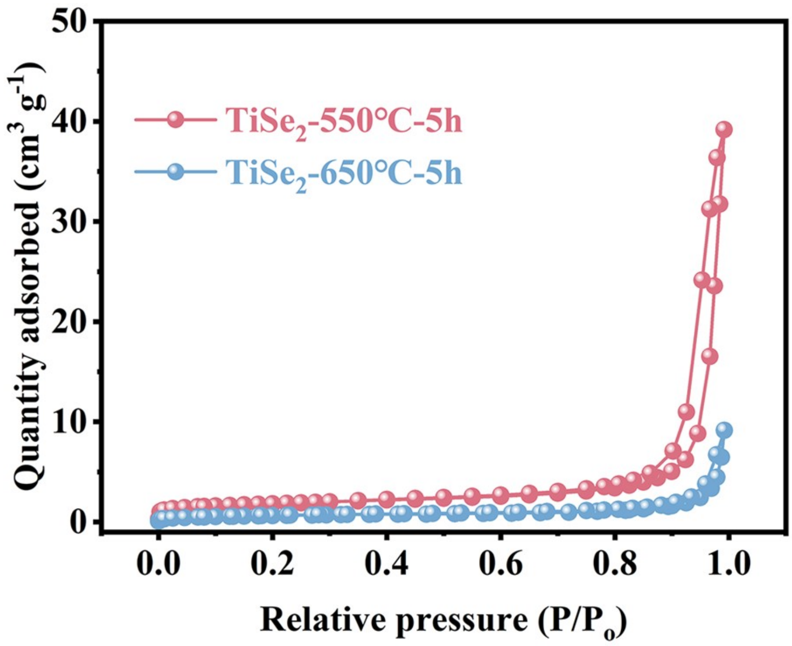

Figure S8. N_2 adsorption−desorption isotherms of $TiSe_2$-550℃-5h and $TiSe_2$-650℃-5h.

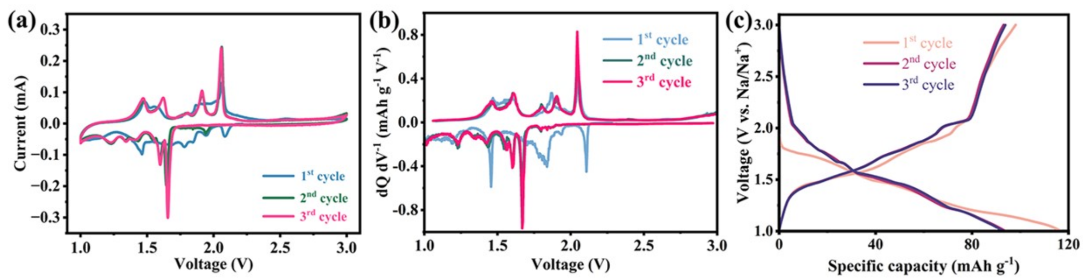

Figure S9. (a) CV curves of $TiSe_2$-550℃-5h, (b) Differential capacitance curves in the first three cycles, (c) initial three GCD curves for $TiSe_2$-650℃-5h at 0.1 A g^{-1}.

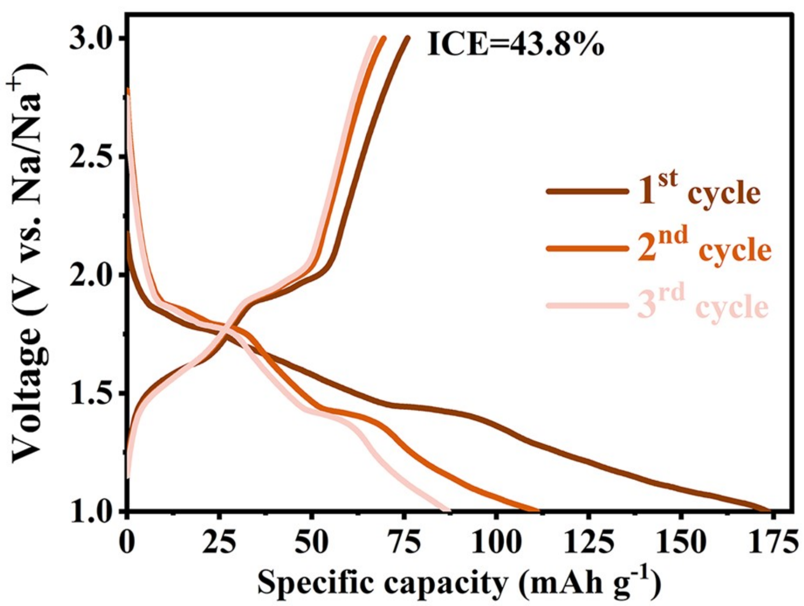

Figure S10. GCD curves of $TiSe_2$-550℃-5h in ester electrolyte (1M $NaPF_6$ in propylene carbonate with 5% fluoroethylene carbonate).

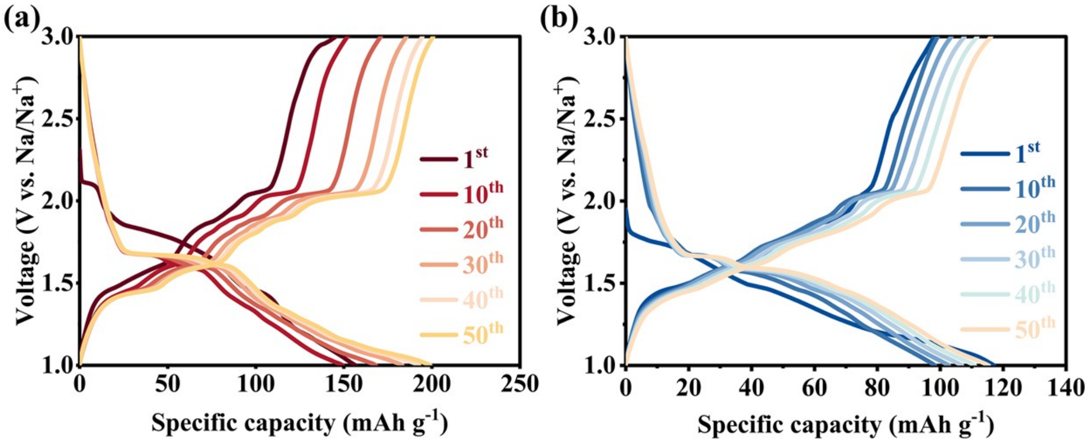

Figure S11. GCD curves at different cycles for (a)$TiSe_2$-550℃-5h and (b)$TiSe_2$-650℃-5h.

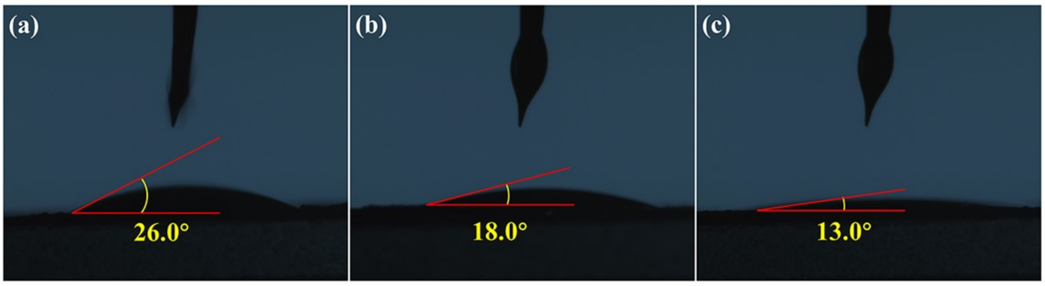

Figure S12. Contact angle between $TiSe_2$-550℃-5h and electrolyte after (a) 0, (b) 25, and (c) 50 cycles.

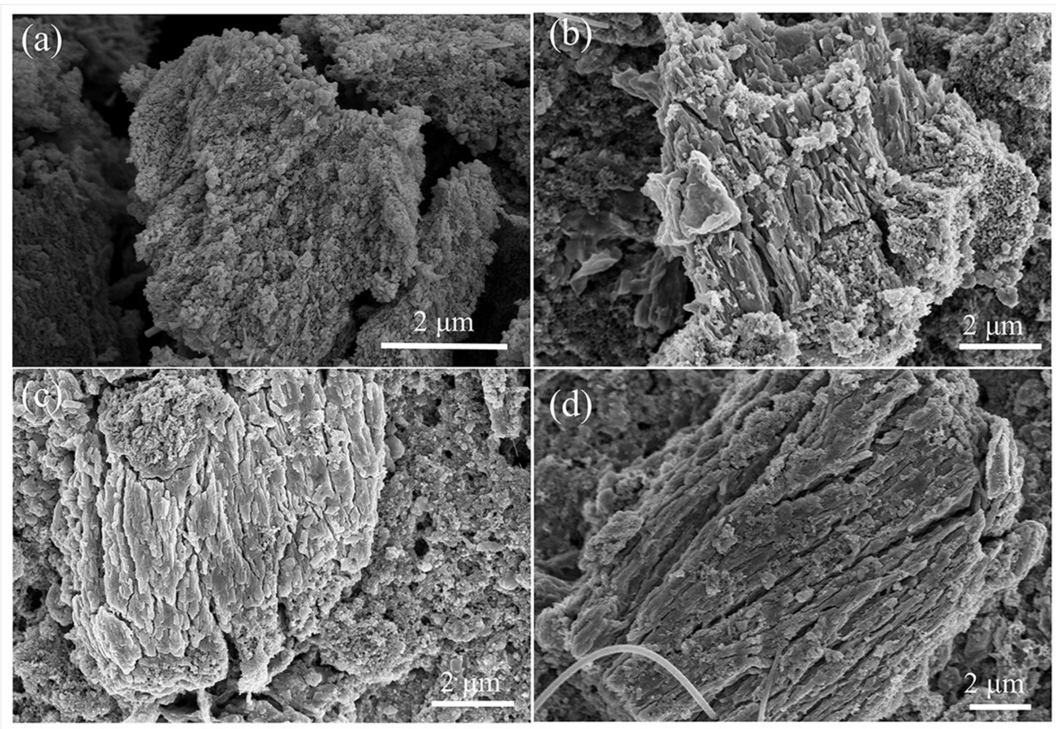

Figure S13. SEM images of $TiSe_2$-550℃-5h after (a) 0, (b) 1, (c) 10, and (d) 50 cycles.

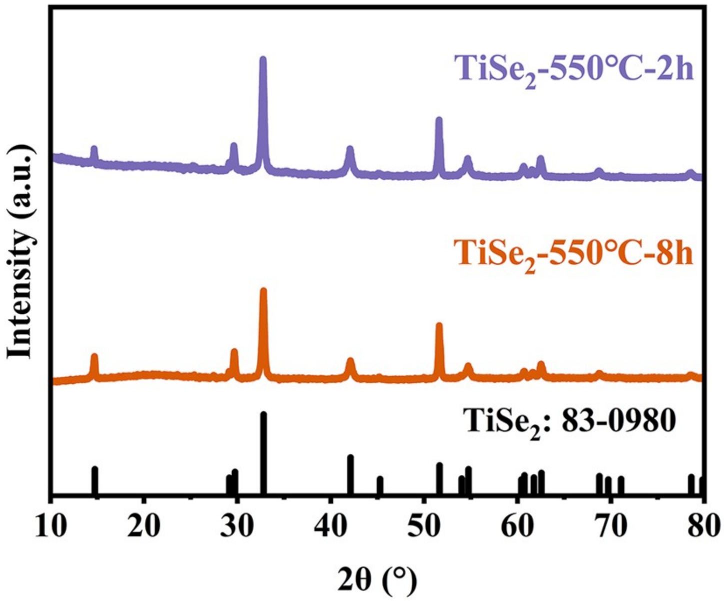

Figure S14. XRD patterns of $TiSe_2$-550℃-2h and $TiSe_2$-550℃-8h.

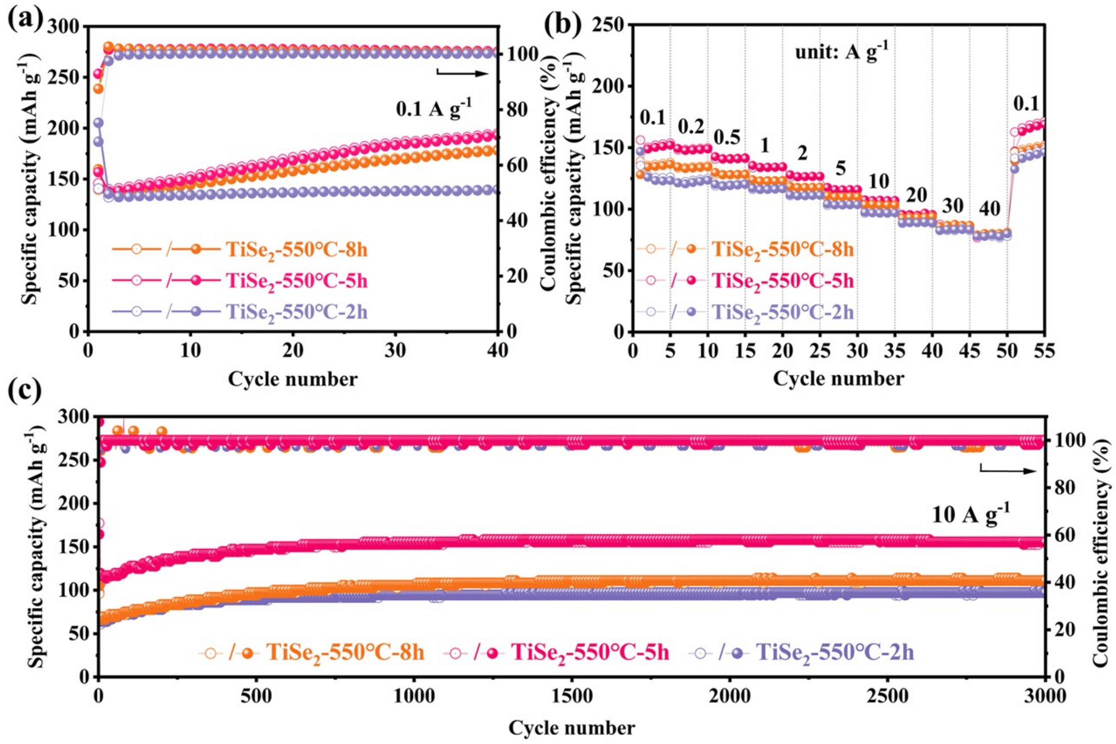

Figure S15. (a) Cycling performance at 0.1 A g^{-1}, (b) rate performance, and (c) long cycling performance at 10 A g^{-1} of $TiSe_2$ calcined at 550 ℃ for different times.

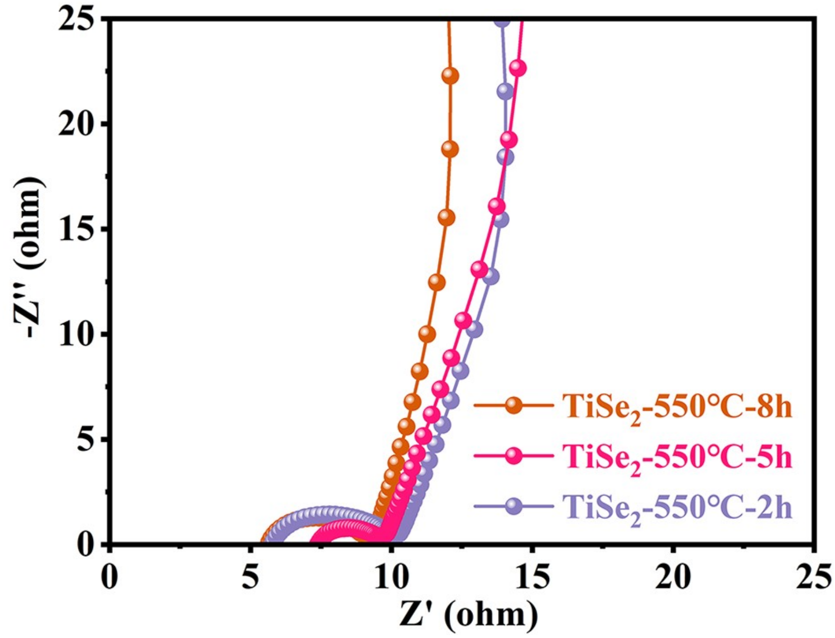

Figure S16. Nyquist plots of $TiSe_2$ calcined at different times for 550 °C.

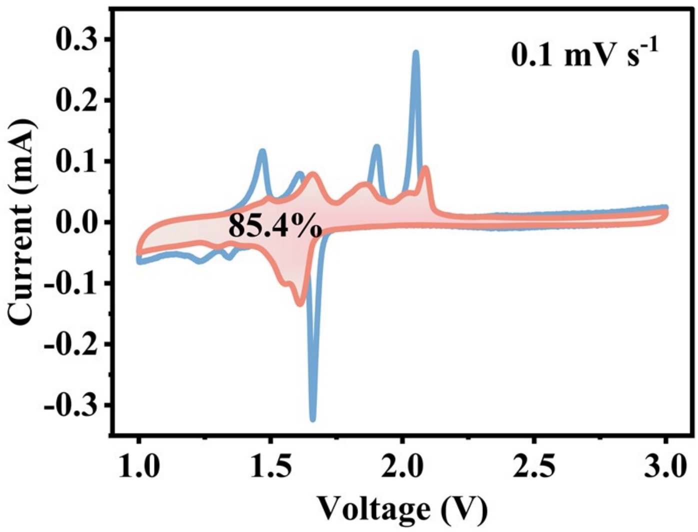

Figure S17. Capacitive controlled portion at 0.1 mV s^{-1}.

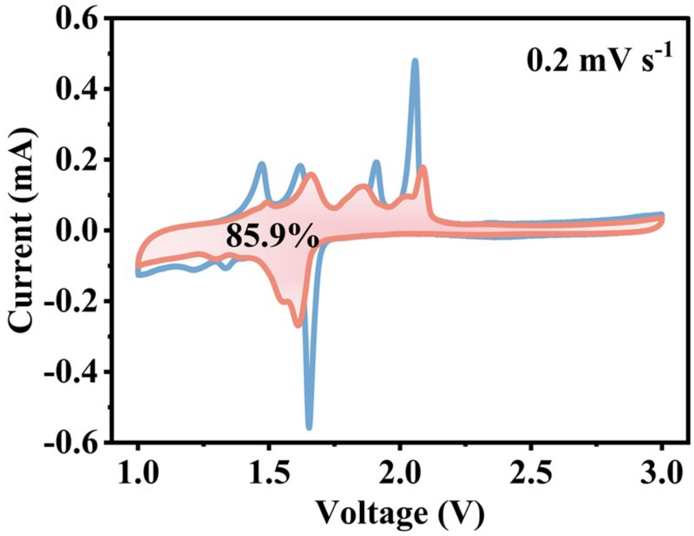

Figure S18. Capacitive controlled portion at 0.2 mV s^{-1}.

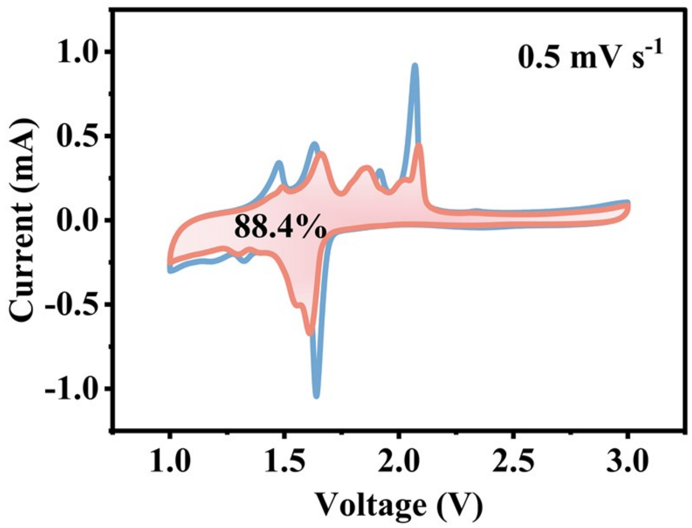

Figure S19. Capacitive controlled portion at 0.5 mV s^{-1}.

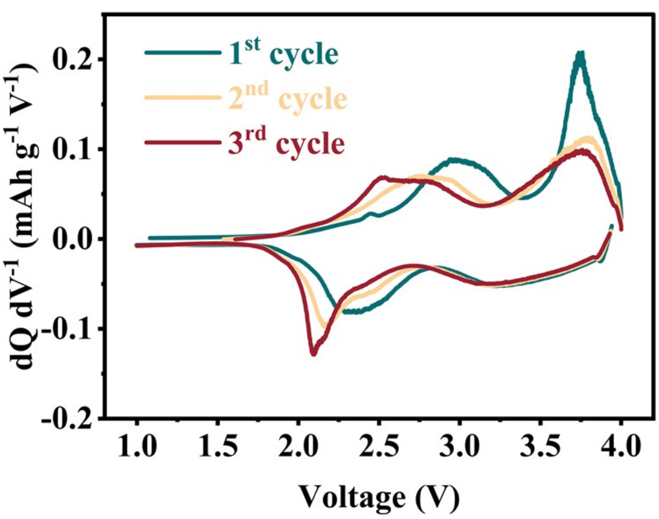

Figure S20. The dQ/dV curves of full-cell at 0.1 A g^{-1} and 25 °C.

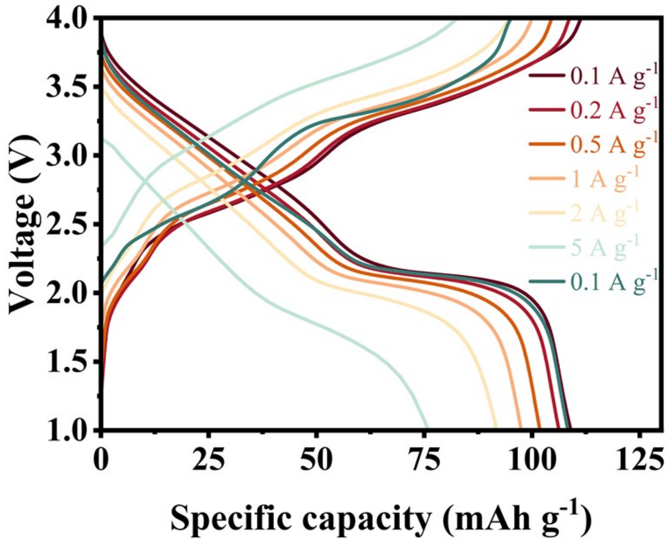

Figure S21. GCD curves in a full battery at different current densities and 25 °C.

Table S1. Cycling performance of $TiSe_2$ and other reported selenides.

Samples	Current density ($A\ g^{-1}$)	Cycle number	Specific capacity ($mAh\ g^{-1}$)	Ref.
$TiSe_2$	10	3000	150	This work
SnSe NSCs	5	100	70	39
BiSe@C	0.2	1000	94	40
ZnSe	4	300	51	41
ZnSe@CeO_2	2	2000	113	42
VSe	2	900	45	43
MnSe	0.5	1000	25	44
NbSe	0.1	100	98	45
TiSe	0.5	300	115	46
Bulk WSe_2	1	1500	8.9	47
ZnSe@NC	10	3000	109	48
$MoSe_2$	5	3000	51	49